The Astrophysical Journal, 764:121 (6pp), 2013 February 20 doi:10.1088/0004-637X/764/2/121

CENTAURUS A AS A POINT SOURCE OF ULTRAHIGH ENERGY COSMIC RAYS

Hang Bae Kim
Department of Physics and The Research Institute of Natural Science, Hanyang University, Seoul 133-791, Republic of Korea; hbkim@hanyang.ac.kr
Received 2012 June 22; accepted 2012 December 19; published 2013 January 30

ABSTRACT

We probe the possibility that Centaurus A (Cen A) is a point source of ultrahigh energy cosmic rays (UHECRs) observed by Pierre Auger Observatory (PAO), through the statistical analysis of the arrival direction distribution. For this purpose, we set up the Cen A dominance model for the UHECR sources, in which Cen A contributes the fraction f_C of the whole UHECR with energy above 5.5×10^{19} eV and the isotropic background contributes the remaining $1 - f_C$ fraction. The effect of the intergalactic magnetic fields on the bending of the trajectory of Cen A originated UHECRs is parameterized by the Gaussian smearing angle θ_s. For the statistical analysis, we adopted the correlational angular distance distribution (CADD) for the reduction of the arrival direction distribution and the Kuiper test to compare the observed and the expected CADDs. We identify the excess of UHECRs in the Cen A direction and fit the CADD of the observed PAO data by varying two parameters f_C and θ_s of the Cen A dominance model. The best-fit parameter values are $f_C \approx 0.1$ (the corresponding Cen A fraction observed at PAO is $f_{C,PAO} \approx 0.15$, that is, about 10 out of 69 UHECRs) and $\theta_s = 5^\circ$ with the maximum likelihood $L_{max} = 0.29$. This result supports the existence of a point source smeared by the intergalactic magnetic fields in the direction of Cen A. If Cen A is actually the source responsible for the observed excess of UHECRs, the rms deflection angle of the excess UHECRs implies the order of 10 nG intergalactic magnetic field in the vicinity of Cen A.

Key words: cosmic rays – galaxies: active – methods: statistical

Online-only material: color figures

1. INTRODUCTION

The origin of the ultrahigh energy cosmic rays (UHECRs) is a long-standing puzzle (Nagano & Watson 2000). The recent confirmation of the Greisen–Zatsepin–Kuzmin (GZK) suppression in the cosmic-ray energy spectrum (Abraham et al. 2008b; Abbasi et al. 2008a; AbuZayyad et al. 2012) implies that UHECRs with energies above the GZK cutoff, $E_{GZK} \sim 4 \times 10^{19}$ eV, mostly come from relatively close extragalactic sources within the GZK radius $r_{GZK} \sim 100$ Mpc. Furthermore, UHECRs with these energies are expected not to be strongly affected by the galactic or extragalactic magnetic field, so that their arrival directions keep some correlation with the source distribution and can be used to trace the sources of UHECRs. Recently Pierre Auger Observatory (PAO) released the updated UHECR data with energy $E \geqslant 5.5 \times 10^{19}$ eV (Abreu et al. 2010). These data can be used for tracing the distribution of UHECR sources through the statistical analysis of the arrival direction distribution. Beginning with the report of the correlation between UHECRs and active galactic nuclei (AGNs) by the PAO collaboration (Abraham et al. 2007, 2008a; Abreu et al. 2010), several attempts were made to identify the UHECR sources. Most attempts aimed to test the plausibility of a certain kind of high-energy astrophysical object whose number ranges from a few to a few hundred (Takami et al. 2009a, 2009b; Cuesta & Prada 2009; Koers & Tinyakov 2009; Kashti et al. 2008; Abbasi et al. 2006, 2008b). In this paper, we aim to test the other extreme possibility that a single dominating source is responsible for the large part of observed UHECRs.

The most frequently mentioned candidates for UHECR source are Centaurus A (Cen A) and Messier 87 (M87) in the Virgo Cluster, which are active galaxies very close to us. Many people suggested that Cen A might be the source of UHECRs (Romero et al. 1996; Anchordoqui et al. 2001; Isola et al. 2002; Hardcastle et al. 2009; Honda 2009; Gopal-Krishna et al. 2010; Fraija et al. 2010; Anchordoqui et al. 2011). Cen A is located in the southern sky, near the center of the exposure region of the PAO experiment. Therefore, the PAO data provide the best chance for checking whether Cen A is a strong source of UHECRs. Actually, the correlation of UHECRs with AGNs was strengthened by many UHECRs observed around Cen A. On the contrary, the number of UHECRs around M87 is smaller than the expected one considering its distance, weakening the claimed AGN correlation. Our purpose is to quantify the Cen A contribution in the observed UHECR by PAO and thus try to establish the existence of a point source in the Cen A direction.

For a single dominating source to be able to explain the large portion of UHECR data, the intergalactic magnetic fields must play a significant role, spreading UHECRs over the large region of the sky around the source. Unfortunately, our knowledge about the intergalactic magnetic fields is rather poor yet. Modeling the intergalactic magnetic fields has its own uncertainty. For this reason, we choose a different and simpler strategy. We parameterize the effect of intergalactic magnetic fields on the deflection of UHECR trajectory by the Gaussian spreading of UHECR arrival directions around the source. In addition, we also need to consider the contribution from other sources to explain the whole set of observed UHECR arrival directions. For this purpose, we introduce one more parameter measuring the fraction of Cen A contribution to observed UHECRs. Then, we search for the values of two parameters with which the observed UHECR arrival directions can be plausibly explained through the statistical comparison of the arrival direction distributions.

Statistical comparison of the arrival direction distributions can be done in many different ways. In Kim & Kim (2011, 2012), we developed the statistical test methods, whose basic idea is that the two-dimensional distribution of arrival directions is reduced to the one-dimensional probability distributions, which can be compared by using the well-known Kolmogorov–Smirnov

(K-S) test or its variants. We proposed a few reduced one-dimensional distributions suitable for the test of correlation between the UHECR arrival directions and the point sources. Among them, we adopt the correlational angular distance distribution (CADD) method, which will be briefly described in Section 3.

This paper is organized as follows. In Section 2, we explain the Cen A dominance model for the UHECR sources and the details needed for the Monte Carlo simulations of UHECR arrival directions. In Section 3, we briefly introduce our statistical methods for comparing two arrival direction distributions. In Section 4, the results of our analysis are presented. We give a few discussions on the results and conclude in Section 5.

2. THE SINGLE DOMINATING SOURCE MODEL FOR UHECRs

We examine the plausibility of the idea that the Cen A is the dominant source of UHECRs through the statistical analysis of the arrival direction distribution of UHECRs. For more definite interpretation of our analysis, we need to solidify the UHECR source model with the Cen A dominance and the method adopted for statistical analysis. In this section, we describe the details of the Cen A dominance model for the UHECR source.

Cen A is located at $\alpha = 201.^\circ37, \delta = -43.^\circ02$ in the equatorial coordinates, and the distance is estimated to be 3–5 Mpc (Harris et al. 2010). We consider Cen A as a smeared point source of UHECRs. This is mainly to incorporate the fact that the trajectories of UHECRs can be bent by intervening magnetic fields. We may model the intervening galactic and extragalactic magnetic fields between Cen A and the Earth, but it would involve large arbitrariness due to our lack of knowledge on extragalactic magnetic fields. Instead of detailed modeling of magnetic fields, we simply assume that Cen A has a Gaussian flux distribution on the sky with a certain angular width θ_s, called the smearing angle, so that the effect of magnetic fields is measured through it. Then the UHECR flux at a direction $\hat{\mathbf{r}}$ contributed by Cen A can be written as

$$F_{\rm CA}(\hat{\mathbf{r}}) = \overline{F}_{\rm CA}\frac{\exp[-(\theta(\hat{\mathbf{r}})/\theta_s)^2]}{N(\theta_s)}, \tag{1}$$

where $\overline{F}_{\rm CA}$ is the averaged flux of Cen A, $\theta(\hat{\mathbf{r}}) = \cos^{-1}(\hat{\mathbf{r}}\cdot\hat{\mathbf{r}}_{\rm CA})$ is the angle between the direction $\hat{\mathbf{r}}$ and Cen A, and $N(\theta_s) = (1/4\pi)\int d\Omega \exp[-(\theta(\hat{\mathbf{r}})/\theta_s)^2]$ is the normalization constant of the smearing function. For small θ_s, $N(\theta_s) \approx \theta_s^2/4$, and for large θ_s, $N(\theta_s) \approx 1$. For the small smearing angle θ_s, the average deflection angle is $\langle\theta\rangle \equiv \int \theta e^{-(\theta/\theta_s)^2} d\Omega / \int e^{-(\theta/\theta_s)^2} d\Omega \approx \theta_s$, and the rms deflection angle is $\theta_{\rm rms} \equiv \sqrt{\langle\theta^2\rangle} \approx 1.12\theta_s$.

Though Cen A can be a dominant source of UHECRs, it is very unlikely that Cen A is the only source of UHECRs. We need to consider the contribution from other distributed sources. We consider, for the sake of simplicity, that a certain fraction of UHECRs are originated from Cen A, while the remaining fraction of them are from the isotropically distributed background contributions. Then, the expected flux at a given arrival direction $\hat{\mathbf{r}}$ is the sum of two contributions,

$$F(\hat{\mathbf{r}}) = F_{\rm CA}(\hat{\mathbf{r}}) + F_{\rm ISO}. \tag{2}$$

Now we define the Cen A fraction $f_{\rm C}$ to be

$$f_{\rm C} = \frac{\overline{F}_{\rm CA}}{\overline{F}_{\rm CA} + F_{\rm ISO}}. \tag{3}$$

The UHECR flux can be written as

$$F(\hat{\mathbf{r}}) = f_{\rm C}\overline{F}\frac{\exp[-(\theta(\hat{\mathbf{r}})/\theta_s)^2]}{N(\theta_s)} + (1 - f_{\rm C})\overline{F}, \tag{4}$$

where $\overline{F} = \overline{F}_{\rm C} + F_{\rm ISO}$. Out of three parameters $\overline{F}_{\rm C}$, $F_{\rm ISO}$, and θ_s, the Cen A fraction $f_{\rm C}$ and the smearing angle θ_s are treated as the free parameters of the model, while the average flux $\overline{F}$ is fixed by the total number of UHECR events.

To do the simulation for the observed arrival directions of UHECRs, we also need to take into account the efficiency of the detector as a function of the arrival direction. It depends on the location and the characteristics of the detector array. Here, we consider only the geometric efficiency, which is determined by the location of the detector and the zenith angle cut of the data. Then the exposure function $h(\hat{\mathbf{r}})$ depends only on the declination δ,

$$h(\delta) = \frac{1}{\pi}\left[\sin\alpha_m \cos\lambda\cos\delta + \alpha_m \sin\lambda\sin\delta\right], \tag{5}$$

where λ is the latitude of the detector array, θ_m is the zenith angle cut, and

$$\alpha_m = \begin{cases} 0, & \text{for } \xi > 1, \\ \pi, & \text{for } \xi < -1, \\ \cos^{-1}\xi, & \text{otherwise.} \end{cases} \quad \text{with } \xi = \frac{\cos\theta_m - \sin\lambda\sin\delta}{\cos\lambda\cos\delta}.$$

The expected flux at the detector array is proportional to $F(\hat{\mathbf{r}})h(\hat{\mathbf{r}})$. We also note that the Cen A fraction $f_{\rm C}$ is the fraction of Cen A contribution over the whole sky. It is in general different from the fraction of Cen A contribution within the sky covered by a given detector array, because the latter is masked by the exposure function. We denote the latter, e.g., for PAO, by $f_{\rm C,PAO}$ to distinguish it from the former.

3. STATISTICAL COMPARISON OF TWO ARRIVAL DIRECTION DISTRIBUTIONS

We now turn to the statistical method to measure the plausibility of the Cen A dominance model. In Kim & Kim (2011, 2012), we developed the simple comparison method for the UHECR arrival direction distributions, where the two-dimensional UHECR arrival direction distributions on the sphere are reduced to one-dimensional probability distributions of some sort, so that they can be compared by using the standard K-S test or its variants. In this paper, we adopt the reduction methods called the CADD. For a detailed explanation of this method, see Kim & Kim (2011, 2012). Here, we briefly present the basic ideas of these distributions and how to calculate the probability measuring the plausibility.

CADD is the probability distribution of the angular distances of all pairs of UHECR arrival directions and the point-source directions, $\theta_{ij'} \equiv \cos^{-1}(\hat{\mathbf{r}}_i \cdot \hat{\mathbf{r}}'_j)$, where $\hat{\mathbf{r}}_i$ $(i = 1, \ldots, N)$ are the UHECR arrival directions, $\hat{\mathbf{r}}'_j$ $(j = 1, \ldots, M)$ are the point-source directions, and N and M are their total numbers, respectively. From the given point-source set and the UHECR arrival direction data set, we can get CADD. Then, we can apply the K-S test or its variants, such as the Kuiper test and Anderson–Darling test, to compare two CADDs, one from the observed UHECR data set and the other from the expected (simulated) UHECR data set from the model under consideration. In this analysis, we use the Kuiper (KP) test because its sensitivity is found to be most appropriate for our

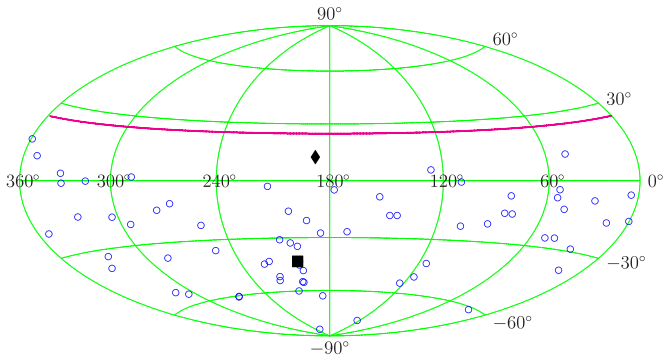

Figure 1. Distribution of the arrival directions of 69 UHECRs, represented by blue circles (○), with energy $E \geqslant 5.5 \times 10^{19}$ eV reported by PAO in 2010, in the equatorial coordinates plotted using the Hammer projection. The solid red line represents the exposure boundary of the PAO experiment. The locations of Cen A (■) and M87 (♦) are also shown for reference.

(A color version of this figure is available in the online journal.)

purpose and the probability function of its statistic is available in analytic form. The KP test is based on the cumulative probability distribution (CPD), $S_N(x) = \int^x p(x')dx'$, and the KP statistic is the sum of maximum differences above and below two CPDs,

$$D_{\rm KP} = \max_x [S_{N_1}(x) - S_{N_2}(x)] + \max_x [S_{N_2}(x) - S_{N_1}(x)]. \quad (6)$$

From the KP statistic $D_{\rm KP}$, the probability that CADD of the observed data is obtained from the model under consideration can be estimated using the Monte Carlo simulations in general. For the KP statistic $D_{\rm KP}$, when the data in the distribution are all independently sampled, the following approximate probability formula is available:

$$P(D_{\rm KP}|N_e) = Q_{\rm KP}([\sqrt{N_e} + 0.155 + 0.24/\sqrt{N_e}]D_{\rm KP}), \quad (7)$$

where $Q_{\rm KP}(\lambda) = 2\sum_{j=1}^{\infty}(4j^2\lambda^2 - 1)e^{-2j^2\lambda^2}$ and $N_e = N_1N_2/(N_1+N_2)$ is the effective number of data. For CADD, the number of data in the distribution is the number of UHECR data times the number of point sources. Thus, for a single source case, the number of data in CADD is the same as the number of UHECR data. This means that the data in CADD are all independent, and we can use formula (7). Now, $N_1 = N_{\rm O}$ is the number of observed UHECR data and $N_2 = N_{\rm S}$ is the number of mock UHECR data. We can make the expected distribution more accurate by increasing the number of mock data $N_{\rm S}$. In the limit $N_{\rm S} \to \infty$, the effective number of data is simply $N_e = N_{\rm O}$.

4. THE RESULTS OF STATISTICAL TESTS

For the observed UHECR data set, we use the UHECR data released by PAO in 2010 (Abreu et al. 2010). It contains 69 UHECRs with energy higher than 5.5×10^{19} eV. The PAO site has the latitude $\lambda = -35.^\circ 20$, and the zenith angle cut of the released data is $\theta_m = 60^\circ$. The arrival directions of the released PAO data are shown in Figure 1. The locations of Cen A and M87 are also marked for reference. For the correlation test between the UHECR arrival directions and the astrophysical objects, the choice of the energy cut can be crucial. For low-energy UHECRs, the effects of intergalactic magnetic fields may be so strong that the correlation of UHECR arrival directions with their sources can be completely erased. The energy cut 5.5×10^{19} eV of the released data was chosen to be higher enough than the GZK cutoff so that their sources can be restricted within the GZK radius ∼100 Mpc. This value of the energy cut is good enough for correlation analysis. Thus, we use the full set of released PAO data for our analysis.

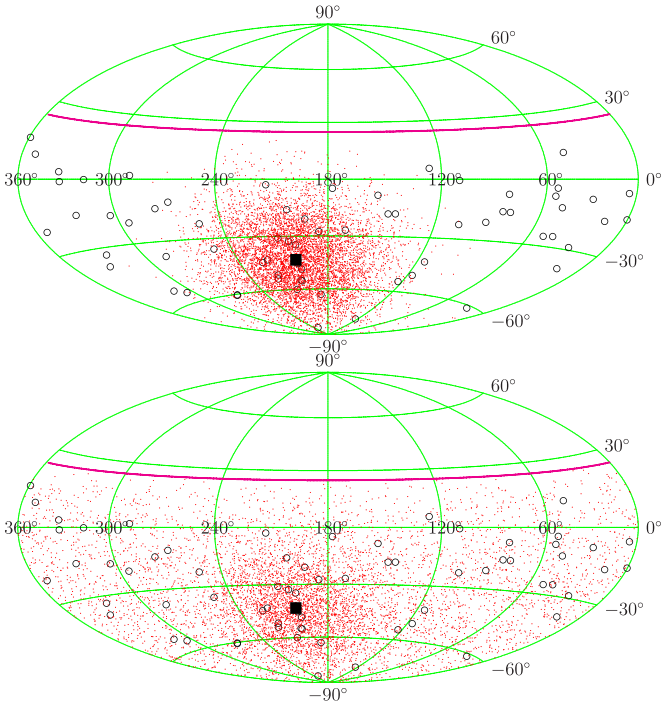

Figure 2. Distributions of the mock UHECR arrival directions (6900 events, represented by small red dots) for the PAO experiment, obtained from the Cen A dominance model for two different values of the Cen A fraction $f_{\rm C} = 1.0$ and $f_{\rm C} = 0.3$ with the smearing angle $\theta_s = 30^\circ$.

(A color version of this figure is available in the online journal.)

From the Cen A dominance model, the expected arrival direction distribution can be obtained through the simulation. As an illustration, we show the arrival direction distributions of 6900 mock UHECRs for two different values of the Cen A fraction, $f_{\rm C} = 1.0$ and $f_{\rm C} = 0.3$ with the same smearing angle $\theta_s = 30^\circ$ in Figure 2. From the observed UHECR set and the mock UHECR set, we obtain the observed and the expected CADDs as described in the previous section and calculate the KP statistic using Equation (6). To obtain the KP statistic with sufficient accuracy, we generate 10^6 mock UHECR events. Though we still have small fluctuations in the KP statistic for this number of mock events, the accuracy is sufficient for our purpose. Then, the probability is calculated by using Equation (7). We also checked the probability by direct Monte Carlo simulation for several cases and confirmed that Equation (7) is good enough.

Figure 3 shows CADDs and their CPDs of the PAO data, the isotropic distribution, and two cases of the Cen A dominance model. Close examination of CADD and its CPD is quite useful for understanding the results of statistical analysis and what causes the discrepancy between the data and the prediction of the model. For a single source, CADD is simply the distribution of angular distances of all UHECRs from the source. The CADD of the isotropic distribution has a bell shape, reflecting the relative location of Cen A and the exposure function of the PAO experiment. On the contrary, the CADD of the PAO data has a distinguished peak at small angles, which means that there is an excess of observed UHECRs near Cen A compared to the isotropic distribution. The KP test on CADD indicates that the probability that this excess of the PAO data is obtained from

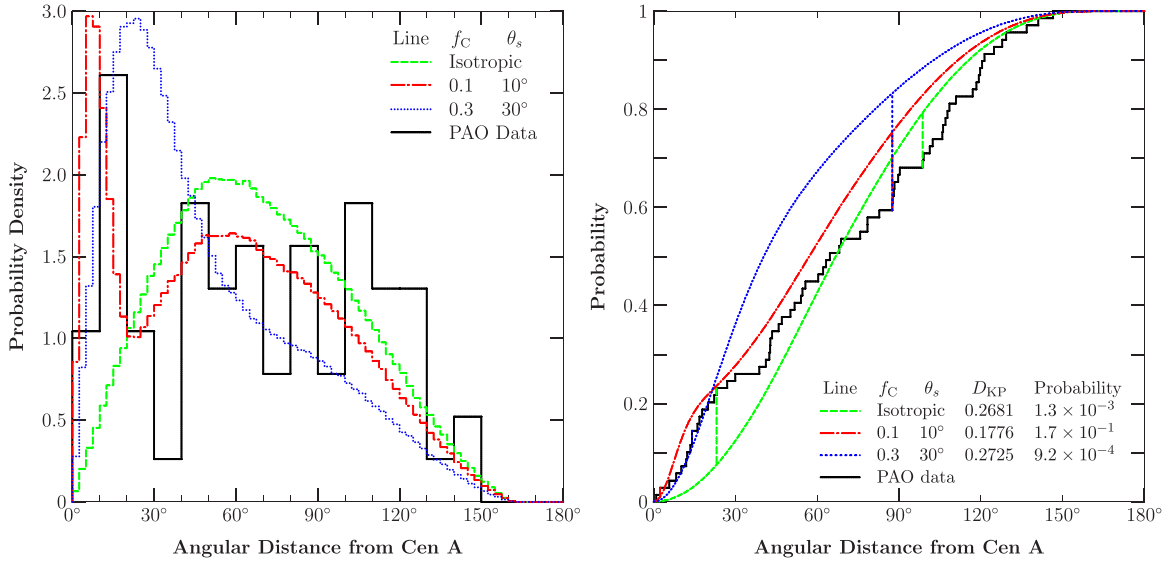

Figure 3. CADDs (left panel) and their CPDs (right panel) of the PAO data, the isotropic distribution, and the Cen A dominance model with the parameter sets ($f_C = 0.1, \theta_s = 10^\circ$) and ($f_C = 0.3, \theta_s = 30^\circ$). Vertical lines in the right panel represent the sizes and the locations of the maximum differences between the CPD of the PAO data and those of the models considered.

(A color version of this figure is available in the online journal.)

the isotropic distribution by chance is 1.3×10^{-3}. Thus, this excess can be attributed to the Cen A contribution.

The Cen A dominance model has two parameters, the Cen A fraction f_C and the smearing angle θ_s, which can be adjusted to fit itself to this excess peak and the remaining bell-shaped body. The Cen A fraction f_C affects the height of the peak at small angles relative to the bell-shaped body at larger angles. The smearing angle θ_s changes the position and width of the peak. As θ_s increases, the Cen A contribution tends to be isotropic and the peak merges into the bell-shaped body. Using the method described in Section 3, we can calculate the probability that CADD of the observed PAO data is obtained from the Cen A dominance model, as a function of two parameters f_C and θ_s. This yields the likelihood function $L(f_C, \theta_s)$. We assume the uniform prior for two parameters. Thus, the posterior is proportional to the likelihood for the parameter range we are considering. We present the result of Bayesian inference in Figure 4.

The best-fit parameters are $f_C \approx 0.1$ and $\theta_s = 5^\circ$, at which the likelihood reaches its maximum value $L_{max} = 0.29$. The maximum likelihood is slightly less than the 1σ bound 0.32. However, this is not so disappointing, if the simplicity of the Cen A dominance model that the distribution of UHECRs that are not contributed by Cen A is assumed to be isotropic is considered. As you can notice from the CPDs in Figure 3, the parameters near the best-fit value fit the CPD at small angles well, but the fit gets poor at large angles where the isotropic contribution dominates. This makes the overall fit a little bit poor. The main cause of this poor fit is the big dip observed at angles 30°–40°, as seen in the CADD of the PAO data in Figure 3. The big dip means the void region of UHECRs at angular distance 30°–40° from Cen A, which is actually observed at the lower right region near the south pole in the skymap of Figure 1. This departure from isotropy due to the void region makes the assumption of isotropic background in the Cen A dominance model a little bit poor, though it is still a valid first approximation. Actually, this makes the best-fit value of the smearing angle smaller than the naively expected value 10°–20° at which the peak of CADD is observed.

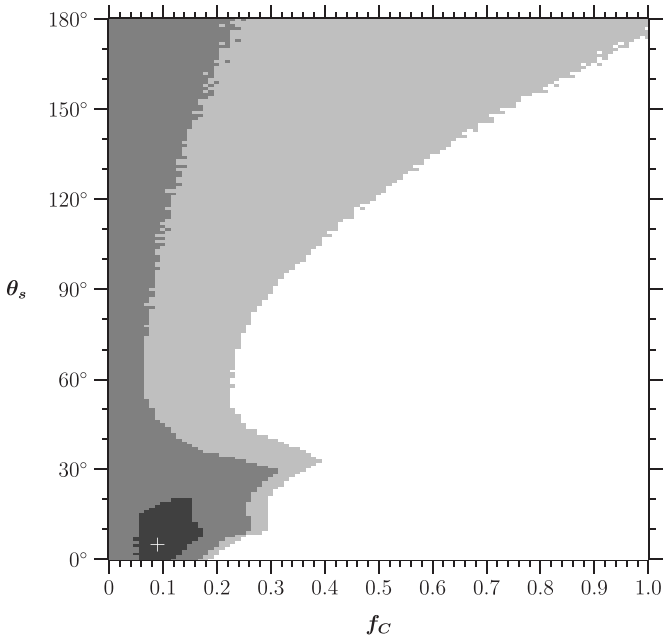

Figure 4. Credible region for the Cen A fraction (f_C) and the smearing angle (θ_s). Gray levels represent the regions for 68%, 95%, and 99.7% confidence levels, respectively. The white + marks the parameter values of the maximum likelihood.

The highest posterior density confidence regions with the 68%, 95%, and 99.7% confidence levels are represented by gray levels in Figure 4. The approximate parameter ranges of 68% confidence level are $0.08 \lesssim f_C \lesssim 0.16$ and $0^\circ \lesssim \theta_s \lesssim 20^\circ$. In Section 2, we mentioned that f_C is different from $f_{C,PAO}$, the fraction of Cen A contribution as observed at the PAO experiment. Because Cen A is located at the central region of the PAO exposure, $f_{C,PAO}$ is larger than f_C. $f_{C,PAO}$ can be obtained as a function of f_C and θ_s when we do the Monte Carlo simulation. In terms of $f_{C,PAO}$, the best-fit value is $f_{C,PAO} = 0.15$ and the 68% confidence level range is $0.10 \lesssim f_{C,PAO} \lesssim 0.25$,

which means that among 69 UHECRs observed by PAO, about 10 ($7 \sim 17$) UHECRs are attributed to Cen A contribution.

5. DISCUSSION AND CONCLUSION

Let us discuss the implications of the results obtained in the previous section. First of all, though we started with the hypothesis that Cen A is a dominant source of UHECRs, what we can actually prove through our statistical analysis is that there is a strong source of UHECRs in the direction of Cen A. To confirm that the actual source is Cen A, other evidences, e.g., from the acceleration mechanism, energetics, or the energy spectrum, are needed.

As seen in the previous section, the major source of uncertainty in our statistical analysis is the assumption that the background contribution is isotropic. We used the UHECR data with energies larger than 5.5×10^{19} eV, which is larger than the GZK cutoff. Thus, their sources are believed to be mostly located within the GZK radius $\sim$100 Mpc, where the matter distribution is not isotropic. One important issue in the UHECR arrival directions is whether the UHECR sources trace the matter distribution. In this regard, it is important to check the existence of the correlation between the UHECR arrival directions and the matter distribution within the GZK radius. There have been several studies on this, and the existence of correlation is not yet conclusive (Koers & Tinyakov 2009; Cuesta & Prada 2009; Takami et al. 2009a). This fact mildly justifies our use of the isotropic background instead of modeling the matter-tracing background. Concerning the background contribution, we again draw your attention to the fact that the CADD of the PAO data depicted in Figure 3 shows the large deficit at the 30°–40° bin and another excess at the 100°–130° range compared to the isotropic distribution. The deficit is due to the void region near the south pole in the PAO data. The chance probability that this void region is obtained from the isotropic distribution is about 5.0×10^{-3} by the same CADD method and KP test. Not only the excess in the Cen A direction but also this void region makes the PAO data anisotropic. Another excess may be due to another point source. We have examined the possibility of the existence of another point source at the region of angular distance 100°–130° from Cen A, but we found that this excess is consistent with isotropy.

The importance of searching for the point sources of UHECRs is that it is the starting point of cosmic-ray astronomy. A known point source of UHECRs can be used to probe the intergalactic magnetic fields in the vicinity of the source. For Cen A, this kind of study was done in Yuksel et al. (2012). Here, we provide the order estimate from our results for comparison. Once we accept the results in the previous section that the fraction $f_{\rm C,PAO} = 0.15$ of the observed UHECRs by PAO is contributed by Cen A and their rms deflection angle is around 10°, we can estimate the rms magnitude of the magnetic fields in the vicinity of Cen A. If we assume that the intergalactic magnetic field is composed of random patches of magnetic fields, the rough estimate for the deflection angle is given by (Nagano & Watson 2000)

$$\delta\theta = 0.8\, Z \left(\frac{E}{10^{20}\,\mathrm{eV}}\right)^{-1} \left(\frac{d\ell_c}{10\,\mathrm{Mpc}^2}\right)^{1/2} \left(\frac{B}{10^{-9}\,\mathrm{G}}\right), \quad (8)$$

where E is the energy of the cosmic-ray particle, d is the size of the magnetic field extension, ℓ_c is the average size of patches, and B is the magnetic field strength. As we discussed in the previous section, the best-fit smearing angle is smaller than the intuitively expected one due to the limitation of our model concerning the isotropic background. The better estimate for the energy and the deflection angle of UHECRs may be obtained by selecting out UHECRs presumably contributed by Cen A. If we select 10 nearest UHECRs from Cen A, the average energy is $E \sim 7.0 \times 10^{19}$ eV, and the rms defection angle is $\delta\theta \sim 10^\circ$ (the maximum deflection angle is $\delta\theta \sim 15^\circ$). Inserting these values together with $Z = 1$ (the proton) and the distance $d \sim 4$ Mpc into Equation (8), we obtain an estimate $B \sim 14\,(\ell_c/\mathrm{Mpc})^{-1/2}$ nG. This gives the rough strength of the intergalactic magnetic field in the vicinity of Cen A.

In conclusion, we examined the possibility that Cen A is a dominant source of UHECRs observed by PAO, by using the statistical analysis of the arrival direction distribution. We set up the Cen A dominance model for the UHECR source, in which Cen A contributes the fraction $f_{\rm C}$ of the whole UHECR with energy above 5.5×10^{19} eV and the isotropic background contributes the remaining fraction $1 - f_{\rm C}$. The effect of the intergalactic magnetic fields on the bending of the trajectory of UHECRs originated from Cen A is parameterized by the Gaussian smearing angle θ_s. We adopted the CADD method for the reduction of the arrival direction distribution and the KP test to compare the observed and the expected CADDs and to estimate the significance level of the similarity. We observed the excess of UHECRs in the Cen A direction in CADD. Then we tried to fit the CADD of the PAO data by varying two parameters $f_{\rm C}$ and θ_s of the Cen A dominance model. The best-fit parameter values are $f_{\rm C} \approx 0.1$ ($f_{\rm C,PAO} \approx 0.15$) and $\theta_s = 5^\circ$ with the maximum likelihood $L_{\rm max} = 0.29$. The 68% confidence level intervals are $0.10 \lesssim f_{\rm C,PAO} \lesssim 0.25$ and $0^\circ \lesssim \theta_s \lesssim 20^\circ$. It supports the existence of a point source in the direction of Cen A, which is smeared by the action of intergalactic magnetic fields. If Cen A is actually the source responsible for the observed excess, the intergalactic magnetic field in the vicinity of Cen A is estimated to be $B \sim 14\,(\ell_c/\mathrm{Mpc})^{-1/2}$ nG from the rms deflection angle of the excess UHECR.

This research was supported by Basic Science Research Program through the National Research Foundation (NRF) funded by the Ministry of Education, Science and Technology (2012R1A1A2008381).

REFERENCES

Abbasi, R. U., Abu-Zayyad, T., Allen, M., et al. (HiRes Collaboration) 2008a, PhRvL, 100, 101101
Abbasi, R. U., Abu-Zayyad, T., Allen, M., et al. (HiRes Collaboration) 2008b, APh, 30, 175
Abbasi, R. U., Abu-Zayyad, T., Amann, J. F., et al. (HiRes Collaboration) 2006, ApJ, 636, 680
Abraham, J., Abreu, P., Aglietta, M., et al. (Pierre Auger Collaboration) 2007, Sci, 318, 938
Abraham, J., Abreu, P., Aglietta, M., et al. (Pierre Auger Collaboration) 2008a, APh, 29, 188
Abraham, J., Abreu, P., Aglietta, M., et al. (Pierre Auger Collaboration) 2008b, PhRvL, 101, 061101
Abreu, P., Aglietta, M., Ahn, E. J., et al. (Pierre Auger Collaboration) 2010, APh, 34, 314
Abu-Zayyad, T., Aida, R., Allen, M., et al. 2012, ApJ, 757, 26
Anchordoqui, L. A., Goldberg, H., & Weiler, T. J. 2001, PhRvL, 87, 081101
Anchordoqui, L. A., Goldberg, H., & Weiler, T. J. 2011, PhRvD, 84, 067301
Cuesta, A. J., & Prada, F. 2009, arXiv:0910.2702
Fraija, N., Sahu, S., & Zhang, B. 2010, arXiv:1007.0455
Gopal-Krishna, B. P. L., de Souza, V., & Wiita, P. J. 2010, ApJL, in press (arXiv:1006.5022)
Hardcastle, M. J., Cheung, C. C., Feain, I. J., & Stawarz, L. 2009, MNRAS, 393, 1041
Harris, G. L. H., Rejkuba, M., & Harris, W. E. 2010, PASA, 27, 457
Honda, M. 2009, ApJ, 706, 1517
Isola, C., Lemoine, M., & Sigl, G. 2002, PhRvD, 65, 023004

Kashti, T., & Waxman, E. 2008, JCAP, 05, 006
Kim, H. B., & Kim, J. 2011, JCAP, 03, 006
Kim, H. B., & Kim, J. 2012, arXiv:1203.0386
Koers, H. B. J., & Tinyakov, P. 2009, JCAP, 04, 003
Nagano, M., & Watson, A. A. 2000, RvMP, 72, 689
Romero, G. E., Combi, J. A., Anchordoqui, L. A., & Perez Bergliaffa, S. E. 1996, APh, 5, 279
Takami, H., Nishimichi, T., & Sato, K. 2009a, PThPh, in press (arXiv:0910.2765)
Takami, H., Nishimichi, T., Yahata, K., & Sato, K. 2009b, JCAP, 06, 031
Yuksel, H., Stanev, T., Kistler, M. D., & Kronberg, P. P. 2012, ApJ, 758, 16